Progress In Electromagnetics Research Letters, Vol. 102, 77–85, 2022

Compact and Broadband Uniplanar Microstrip Antenna for Endfire Radiation

Rajbala*

Abstract—A compact and broadband uniplanar Microstrip Antenna (MSA) is proposed for endfire radiation at sub-6 GHz 5G frequency band. The proposed antenna consists of a semi-elliptical radiating element and a U-shaped ground plane. The use of semi-elliptical radiating element results in a wide impedance bandwidth (BW) and compact size. The U-shaped ground plane further improves the bandwidth due to the increased coupling from radiating element to ground. An endfire radiation, 3.8 dBi peak gain, and 49.8% BW are achieved while a compact size of $0.47\lambda_0 \times 0.13\lambda_0 \times 0.008\lambda_0$ (where λ_0 is the wavelength in free space at the center frequency) is kept. To validate the simulation results, prototype of the proposed antenna was fabricated and tested. The measured results are in good agreement with the simulated ones.

1. INTRODUCTION

With increased exigency of portable communication systems, the utility of printed antennas has attained a prominent edge over the other types of antennas due to its compactness, low profile, conformability, and cost-effectiveness. A lot of research is going on to design compact and planar antennas by applying concepts of different non-planar antennas. Microstrip antennas provide broadside radiation [1–4]; however, the proposed uniplanar MSA provides endfire radiation. Therefore, literature survey of endfire antennas is provided here to compare the proposed antenna with the literature. Yagi-Uda array, Log-Periodic Dipole Array (LPDA), and Vivaldi antennas provide endfire radiation, and various planar configurations of these antennas are reported in literature to achieve endfire radiation [5–42]. In [5], a balanced antipodal slot-dipole with dual band characteristics is reported with reduced ground plane effect and compact size of $0.21\lambda_L \times 0.21\lambda_L$. A dual band characteristic with omnidirectional and unidirectional patterns in endfire direction is achieved by an aperture-coupled dipole antenna with offset feed [6].

Generally, Yagi antennas and LPDAs are used for higher gain and higher BW, respectively. The gain of Yagi antenna is increased by adding multiple directors [7–10]. A 7-element Microstrip Line (MSL) fed Yagi-Uda antenna with size $2.3\lambda_0 \times 3.11\lambda_0 \times 0.030\lambda_0$ is reported to achieve > 10 dBi gain and > 20 dB Front to Back ratio (F/B) [7]. A Yagi-Uda antenna with printed magnetic-dipoles provides > 10.5 dBi peak gain and approximately 11.7% fractional bandwidth with twelve elements and large ground plane [8]. To further increase the gain, a stacked multilayer configuration of printed Yagi antenna of size $1.55\lambda_0 \times 1.55\lambda_0 \times 0.56\lambda_0$ is reported to achieve 11 dBi gain and 14% fractional bandwidth [9]. A 6-element Yagi with a curved disk monopole as driven element and flat disk monopole as directors provides 20% BW and more than 10 dBi gain [10]. Since feed structure also plays a crucial role for wideband impedance matching, various feed structures are reported in [11–20] for Yagi-Uda antennas to increase the bandwidth. A printed Yagi antenna consisting of a tilted self-complimentary driven element and a triangular notch on ground provides broadband frequency response at the cost of poor F/B [21]. A

Received 2 December 2021, Accepted 12 January 2022, Scheduled 17 January 2022

* Corresponding author: Rajbala (rajbala21@gmail.com).
The author is with the Department of Electrical Engineering, Indian Institute of Technology Bombay, Mumbai, India.

printed quasi-Yagi antenna consisting of a circular-sector fed and two annular-sector director elements provides 10 dBi gain and 17.6% bandwidth [22]. Many different techniques are reported in [23–30] to make the Yagi antenna compact and broadband. A Yagi antenna with multiple reflectors is reported to improve F/B [23]. A printed quasi-Yagi antenna consisting of a fed dipole, two parasitic strips, and modified ground plane is reported to achieve 16.7% bandwidth and 4 dBi gain [24]. To decrease the lateral size of the Yagi antenna, stepped width reflector [25] and U-shaped reflector [26] can be used. A broadband Yagi-based MIMO antenna system with 2 elements and loop excitation is reported to have 45% bandwidth and 6 dBi gain with overall size $0.90\lambda_0 \times 1.44\lambda_0 \times 0.014\lambda_0$ [27]. A 3-element quasi-Yagi antenna having size $0.41\lambda_0 \times 0.54\lambda_0$ is reported to achieve 41.4% bandwidth and 6.5 dBi ± 0.5 dB gain with a reflector and a director, and two-element LPDA as driven element [28]. A 3-element uniplanar Yagi antenna with $0.4\lambda_0 \times 0.36\lambda_0$ size is reported to achieve 4.6% bandwidth and 8.2 dBi gain [29]. A 2-element uniplanar Yagi-MSA with semi-elliptical driven element is reported to achieve 11.3% bandwidth and 5.2 dBi gain with an overall size of $0.50\lambda_0 \times 0.13\lambda_0 \times 0.009\lambda_0$ [30].

Various configurations of broadband LPDAs are reported in [27–38]. To make the LPDAs compact along the lateral dimension, meandered dipoles are used at the cost of reduced gain, and higher X-pols [31–33] or the dipole elements are loaded at the ends of the half dipoles at the cost of decreased gain [34]. The bandwidth of the LPDAs is limited by feed network, so various broadband feed networks are reported in [35–37]. In [35], a balun with two coaxial cables is reported to achieve better phase centre stability. A log-periodic microstrip antenna is reported to achieve 120% impedance bandwidth, 10 dBi peak gain, and improved radiation pattern at lower frequencies due to the mixed MSL feed [36]. An LPDA with a simplified microstrip feed is reported in [37] in which there are crossed dipoles with microstrip line feed on one side of the substrate and crossed dipole connected to parallel microstrip feed line and a truncated ground plane on the other side of the substrate. In [38], a mode converter balun is reported for an ultra-broadband LPDA. A wideband LPDA can be designed using bow-tie dipole elements [39]. A conformal LPDA with trapezoidal bow-tie elements is reported to achieve 118% bandwidth and 5 dBi average gain [40]. A combination of hat-loaded and T-loaded dipole elements are used to design a compact and ultra-broadband LPDA antenna [41]. A SIW fed clamped-mode LPDA with non-resonant metamaterial structure on both sides of the substrate is used to increase the gain of the antenna [42].

In this paper, a compact and broadband uniplanar MSA with a semi-elliptical radiating patch and U-shaped ground plane is proposed for endfire radiations. The semi-elliptical radiating patch is used to achieve wide BW and compact size along the antenna axis, and the U-shaped ground plane is used to reduce the lateral dimension. Additionally, the bent ground plane improves the BW due to the increased coupling from radiating patch to the ground.

2. ANTENNA DESIGN, EVOLUTION PROCEDURE AND ANALYSIS

2.1. Antenna Design

Figure 1 presents the geometry of the proposed uniplanar MSA on a substrate with dielectric constant $\varepsilon_r = 2.55$, thickness $h = 0.079$ cm and loss tangent $\tan\delta = 0.018$. The proposed antenna consists of a semi-elliptical radiating patch and a U-shaped ground plane. The ground plane and radiating patch are placed on the same side of the substrate, and a simple feed is provided with the help of an SMA connector to make the antenna uniplanar. The inner and outer conductors of the connector are connected to the radiating patch and ground plane, respectively, and an adhesive tape is placed between the inner conductor and ground plane to ensure that there is no shorting from the inner conductor to the ground plane.

2.2. Evolution Procedure

A uniplanar MSA with a rectangular radiating patch provides narrow BW. Therefore, to increase the BW, rectangular patch is replaced by an elliptical patch (Antenna 1) as shown in Figure 2(a). The dimensional parameters of Antenna 1 designed for sub-6 GHz 5G frequency band are: substrate length $L_s = 4.6$ cm, substrate width $W_s = 2.0$ cm, ground plane length $L_g = 4.5$ cm, ground plane width $W_g = 0.25$ cm, patch length $L_p = 3.7$ cm, patch width $W_p = 1.4$ cm, spacing between ground and

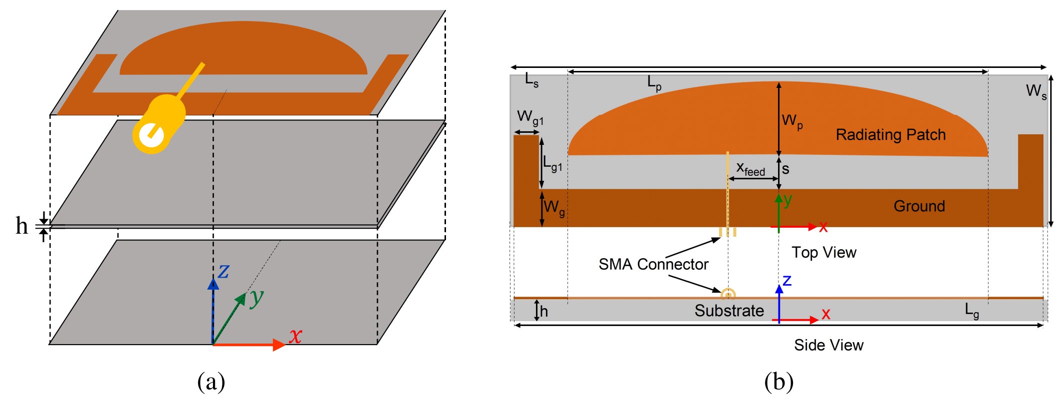

Figure 1. Design of the proposed antenna: (a) layered, and (b) top and side views with geometry parameters.

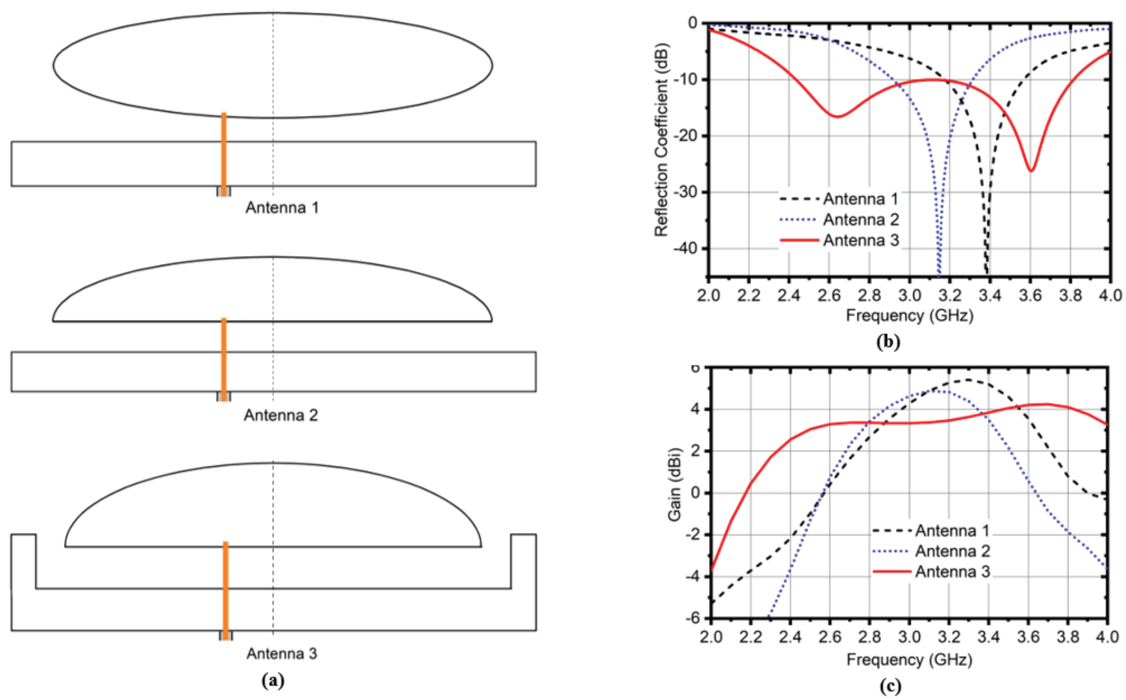

Figure 2. (a) Different stages of the uniplanar MSA: elliptical radiating patch (Antenna 1), semi-elliptical radiating patch (Antenna 2), and semi-elliptical radiating patch and U-shaped ground plane (Antenna 3) and their simulated (b) reflection coefficient (dB), and (c) gain vs frequency plots.

radiating patch $s = 0.25\,\text{cm}$, feed location $x_{feed} = 0.4\,\text{cm}$, and thickness of the annealed copper layer $t = 0.035\,\text{mm}$. The obtained BW and peak gain for Antenna 1 are 11.6% and 5.4 dBi, respectively as shown in Figures 2(b)–(c), and the overall size is $0.52\lambda_0 \times 0.22\lambda_0$. Next, to reduce the size of Antenna 1, half width of the radiating patch is removed (Antenna 2), and all the other dimensional parameters are kept the same. The obtained BW for Antenna 2 is approximately the same as that of Antenna 1. However, the resonance frequency decreases due to the decreased average spacing between the radiating patch and ground plane as compared to Antenna 1. The obtained gain for Antenna 2 is 4.9 dBi, and this decrement in gain is because of the reduced patch width. Next, Antenna 3 is designed by bending the ground plane in a U-shape to further reduce the electrical size of the antenna. The size of the bent part is taken as $L_{g1} = 0.45\,\text{cm}$ and $W_{g1} = 0.15\,\text{cm}$. The U-shaped ground plane also increases the BW due to the increased coupling from radiating element to the ground. Antenna 3 has an electrical size of $0.47\lambda_0 \times 0.13\lambda_0$, and it provides approx. 46% BW and 4.2 dBi peak gain. The simulated $|S_{11}|$ and gain plots of these three antenna configurations are compared in Figures 2(b)–(c).

2.3. Parametric Analysis

To see the effects of variation in size of bent part of the ground plane, a parametric study is carried out with the help of CST-MWS 2017. Initially, the length of bent part of the ground plane L_{g1} is varied by keeping all the other parameters fixed to their optimized values. L_{g1} is increased from 0.15 cm to 0.45 cm in a step size of 0.15 cm, and the simulated results are presented in Figure 3. As seen from Figure 3, there are two resonances, one because of the ground and the other because of the radiating patch. The size of the ground is larger than the patch; therefore, the first resonance (lower frequency) is because of the ground. As L_{g1} increases, the coupling from radiating patch to ground plane increases, and the ground plane starts resonating. The resonance frequency of the ground decreases with increase in L_{g1} (because of the inverse relation of length and resonance frequency of a resonant structure), and there is no significant effect on the second resonance (due to the patch) as shown in Figure 3(a). However, for the second resonance, the deepest point of $|S_{11}|$ increases with the increase in L_{g1} due to the increased resistance for higher values of L_{g1}. Because of these two resonances, operational bandwidth for $|S_{11}| < -10$ dB increases from 2.86–3.64 GHz to 2.43–3.82 GHz, and the peak gain decreases slightly from 4.5 dBi to 4.2 dBi as L_{g1} increases from 0.15 cm to 0.45 cm.

Next, the width of bent part of the ground plane W_{g1} is varied by keeping $L_{g1} = 0.45$ cm and

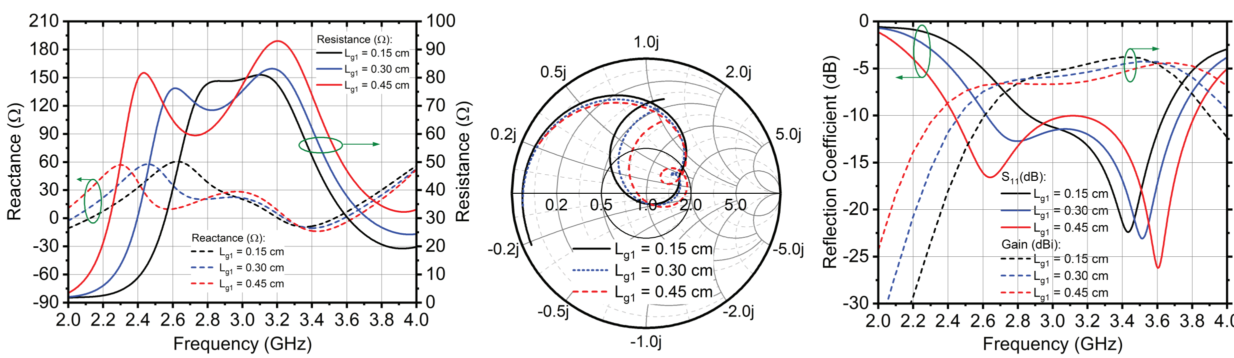

(a) (b) (c)

Figure 3. (a) Input resistance and reactance, (b) Smith chart, and (c) reflection coefficient (dB) and gain (dBi) vs frequency plots of the proposed antenna for $L_{g1} = 0.15$ cm, 0.30 cm and 0.45 cm.

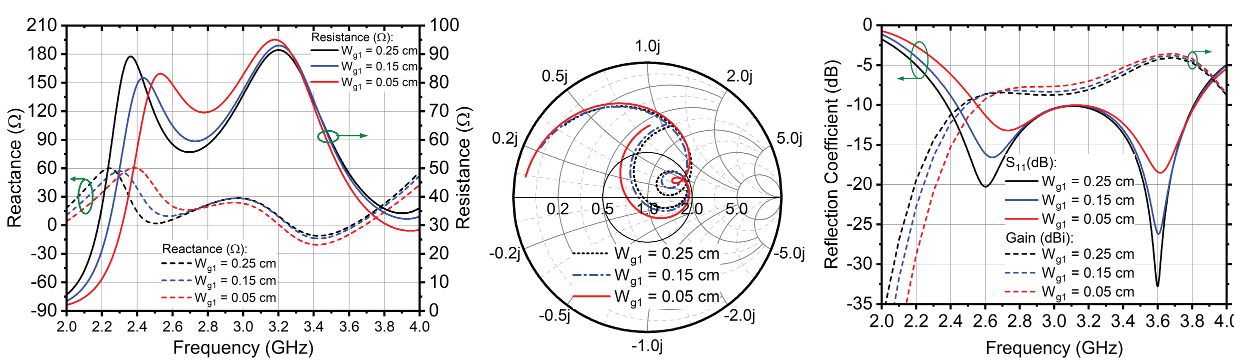

(a) (b) (c)

Figure 4. (a) Input resistance and reactance, (b) Smith chart, and (c) reflection coefficient (dB) and gain (dBi) vs frequency plots of the proposed antenna for $W_{g1} = 0.25$ cm, 0.15 cm and 0.05 cm.

all the other parameters fixed to their optimized values. The width W_{g1} is decreased from 0.25 cm to 0.05 cm in a step size of 0.1 cm, and the simulated results are shown in Figure 4. Since the ground plane length L_g is fixed, if we reduce W_{g1}, then the bent part of the ground plane moves away from the radiating patch which results in reduced coupling from the radiating patch to the ground. This can also be seen from the Smith chart that size of the impedance loop decreases indicating less coupling as W_{g1} decreases. Because of this reduced coupling, the first resonance frequency increases with decrease in W_{g1} whereas there is no significant effect of W_{g1} on the second resonance. Therefore, operational bandwidth for $|S_{11}| < -10$ dB decreases from 2.38–3.82 GHz to 2.55–3.82 GHz, and peak gain increases slightly from 4.2 dBi to 4.3 dBi as W_{g1} decreases from 0.25 cm to 0.05 cm.

2.4. Reasoning for Endfire Radiation

A conventional microstrip antenna provides broadside radiation pattern. However, the proposed uniplanar microstrip antenna (Antenna 3) provides endfire radiation. To demonstrate it, the fringing fields and the radiation pattern at 3.3 GHz are shown in Figure 5. The resultant electric field is in $-x$-direction as seen from the electric field distribution in Figure 5(a). The resultant magnetic field is in $+z$-direction as seen from Figure 5(b). Therefore, in the far-field the electric and magnetic fields will be in $-x$- and $+z$-directions, respectively. The direction of propagation is perpendicular to both electric and magnetic fields for a TEM wave, and the waves travel as a TEM wave in a free space or a far-field. Therefore, the direction of propagation for uniplanar MSA is in $+y$-direction. Since the plane of the antenna is xy-plane and antenna axis along y-axis, the wave propagation is in endfire direction. As shown in Figure 5(c), the radiation pattern at $f = 3.3$ GHz is endfire.

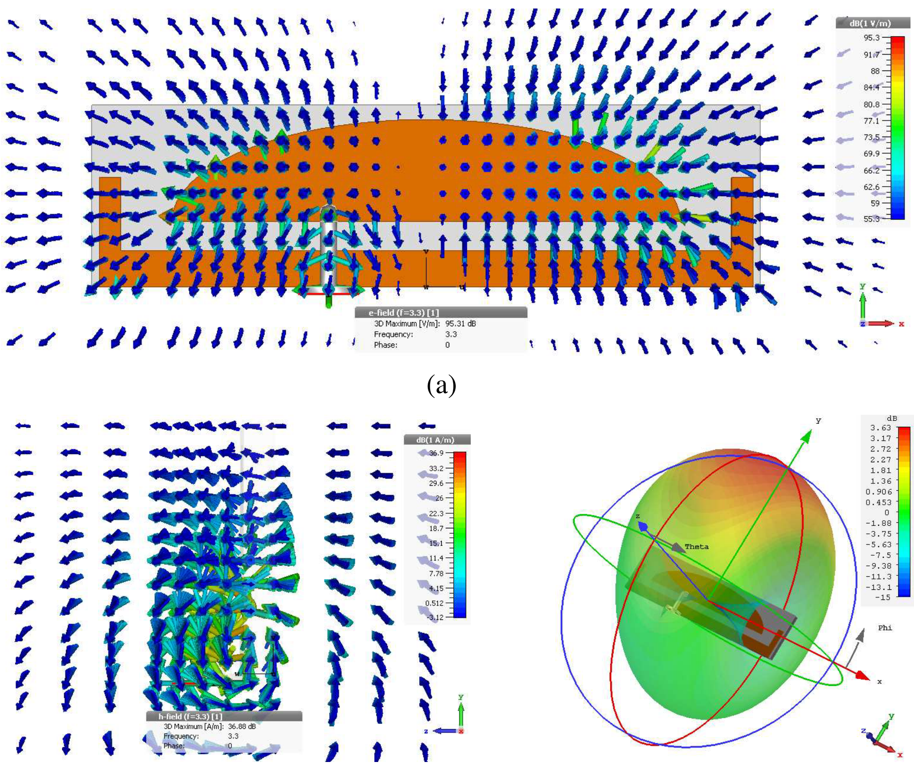

(a) (b) (c)

Figure 5. (a) Electric field, (b) magnetic field, and (c) radiation pattern of the proposed antenna (Antenna 3) at $f = 3.3$ GHz.

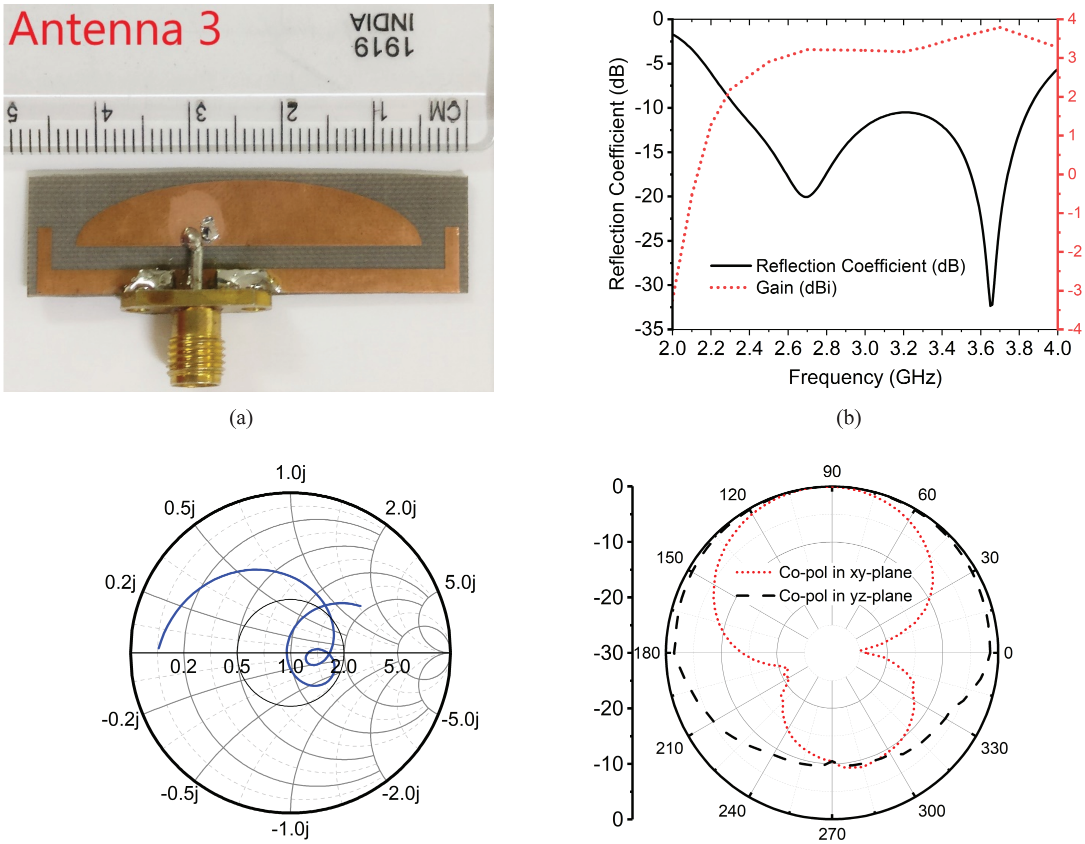

(a) (b)

(c) (d)

Figure 6. (a) Fabricated prototype of the proposed antenna, and its measured results: (b) reflection coefficient (dB) and gain vs frequency plots, (c) input impedance vs frequency plot, and (d) radiation pattern at the centre frequency of operation $f_0 = 3.1\,\text{GHz}$.

3. MEASURED RESULTS AND COMPARISON

The proposed antenna (Antenna 3) is fabricated and tested, and the physical parameters of the antenna are: $L_s = 4.6\,\text{cm}$, $W_s = 1.3\,\text{cm}$, $L_g = 4.5\,\text{cm}$, $W_g = 0.25\,\text{cm}$, $L_{g1} = 0.45\,\text{cm}$, $W_{g1} = 0.15\,\text{cm}$, $L_p = 3.5\,\text{cm}$, $W_p = 0.7\,\text{cm}$, $s = 0.20\,\text{cm}$, and $x_{feed} = 0.67\,\text{cm}$. The prototype of the antenna is shown in Figure 6(a), which is fed by a $50\,\Omega$ SMA-Male connector. The reflection coefficient and Smith chart of the antenna are measured using a vector network analyzer (VNA), and the results are shown in Figures 6(b)–(c). The measured operational BW for $|S_{11}| < -10\,\text{dB}$ is from 2.32 GHz to 3.86 GHz which corresponds to approximately 49.8% BW, and the obtained peak gain is 3.8 dBi. The electrical size of the antenna is $0.47\lambda_0 \times 0.13\lambda_0$ at the centre frequency of operation. The radiation pattern of the proposed antenna at its centre frequency of operation $f_0 = 3.1\,\text{GHz}$ is shown in Figure 6(d). The radiation pattern is endfire with front-to-back ratio of 10.5 dB.

The proposed uniplanar MSA is compared with the literature on the basis of electrical size, percentage bandwidth, gain, front-to-back ratio (F/B), and figure of merit (FoM) as shown in Table 1. The F/B in Table 1 is taken at the centre frequency of operation, and FoM is defined as the ratio of gain bandwidth product and the electrical size of the antenna. For the calculation of gain bandwidth product, the numerical values of gain and percentage bandwidth are considered, and for electrical size, physical size is normalized with respect to the wavelength corresponding to the center frequency of operation. The proposed antenna has a smaller size $(0.47\lambda_0 \times 0.13\lambda_0)$ and provides better FoM with 49.8% bandwidth and a peak gain of 3.8 dBi. Hence, the proposed uniplanar MSA with semi-elliptical radiating patch and U-shaped ground plane can be considered as a good choice for endfire radiation.

Table 1. Comparison of the proposed antenna with previously reported endfire antennas.

Ref. & Year	Description	Size ($\lambda_0 \times \lambda_0$)	BW (%)	Gain (dBi)	F/B (dB)	FoM
[19] - 2016	8-element Quasi-Yagi with folded dipole	0.42×1.16	10.0	9.8	9	196
[20] - 2017	A differential-fed 3-element Yagi with folded dipole and a parasitic stripline resonator	0.53×0.49	12.8	6.5	17	220
[25] - 2016	3-element Yagi with a stepped-width reflector	0.40×0.42	10.5	7.0	17	313
[26] - 2017	4-element Yagi with folded dipole and reflector	0.41×0.42	67.0	5.4	10	1349
[27] - 2017	Array of loop antenna with a director	0.97×1.56	41.4	6.0	18	109
[28] - 2018	3-element Yagi with 2-element LPDA as the driven element	0.54×0.41	41.4	7.0	20	937
[29] - 2019	Uniplanar MSA with a director	0.47×0.36	4.7	8.2	18	183
[42] - 2019	SIW fed Clamped mode LPDA with non-resonant MTM consisting of series of metallic semirings	1.65×2.54	42.4	12.3	19	172
Proposed Work	Uniplanar MSA with U-shaped ground	0.47×0.13	49.8	3.8	10	1955

4. CONCLUSION

A compact and broadband uniplanar microstrip antenna is proposed for endfire radiations. The proposed antenna consists of a semi-elliptical radiating element and U-shaped ground plane. A wide bandwidth and compact size are achieved due to the semi-elliptical radiating element. The U-shaped ground plane further improves the bandwidth due to the increased coupling from radiating element to bent arms of the U-shaped ground plane. The proposed compact antenna having size $0.47\lambda_0 \times 0.13\lambda_0 \times 0.008\lambda_0$ provides a better FoM with 49.8% bandwidth and 3.8 dBi gain. This antenna can be used for sub-6 GHz 5G applications with endfire radiation and can also be integrated easily with RF front-end circuits.

ACKNOWLEDGMENT

The author gratefully acknowledges the support provided by Prof. Sharayu Moharir, Electrical Engineering Department, Indian Institute of Technology Bombay.

REFERENCES

1. Kumar, G. and K. P. Ray, *Broadband Microstrip Antennas*, Artech House, Norwood, MA, 2003.
2. Anguera, J., J. P. Daniel, C. Borja, J. Mumbrú, C. Puente, T. Leduc, N. Laeveren, and P. Van Roy, "Metallized foams for fractal-shaped microstrip antennas," *IEEE Antennas and Propagation Magazine*, Vol. 50, No. 6, 20–38, Dec. 2008.
3. Anguera, J., A. Andújar, S. Benavente, J. Jayasinghe, and S. Kahng, "High-directivity microstrip antenna with mandelbrot fractal boundary," *IET Microwaves, Antennas & Propagation*, Vol. 12, No. 4, 569–575, Mar. 28, 2018.
4. Anguera, J., A. Andújar, and J. Jayasinghe, "High directivity microstrip patch antennas perturbing TModd-0 modes," *IEEE Antennas Wireless Propag. Lett.*, Vol. 19, No. 1, 39–43, 2020.
5. Lu, W.-J., Y.-M. Bo, and H.-B. Zhu, "Novel planar dual-band balanced antipodal slot-dipole composite antenna with reduced ground plane effect," *Int. J. RF and Microwave Comp. Aid. Eng.*, Vol. 22, 319–328, 2012.
6. Xu, J., W.-J. Lu, X.-T. Wu, Y.-M. Bo, L. Zhu, and H.-B. Zhu, "Novel offset-fed dual-band aperture-dipole composite antenna: Operating principle and design approach," *Int. J. RF and Microwave Comp. Aid. Eng.*, Vol. 25, 382–393, 2015.

7. Alhalabi, R. A. and G. M. Rebeiz, "High-gain Yagi-Uda antennas for millimeter-wave switched-beam systems," *IEEE Trans. Antennas Propag.*, Vol. 57, No. 11, 3672–3676, Nov. 2009.
8. Liu, J. and Q. Xue, "Microstrip magnetic dipole Yagi array antenna with endfire radiation and vertical polarization," *IEEE Trans. Antennas Propag.*, Vol. 61, No. 3, 1140–1147, Mar. 2013.
9. Kramer, O., T. Djerafi, and K. Wu, "Vertically multilayer-stacked Yagi antenna with single and dual polarizations," *IEEE Trans. Antennas Propag.*, Vol. 58, No. 4, 1022–1030, Apr. 2010.
10. Hachi, A., H. Lebbar, and M. Himdi, "3D printed large bandwidth new Yagi-Uda antenna," *Progress In Electromagnetics Research Letters*, Vol. 88, 129–135, 2020.
11. Qian, Y., W. R. Deal, N. Kaneda, and T. Itoh, "Microstrip-fed Quasi-Yagi antenna with broadband characteristics," *Electron. Lett.*, Vol. 34, No. 23, 2194–2196, Nov. 1998.
12. Kaneda, N., W. R. Deal, Y. Qian, R. Waterhouse, and T. Itoh, "A broadband planar Quasi-Yagi antenna," *IEEE Trans. Antennas Propag.*, Vol. 50, No. 8, 1158–1160, Aug. 2002.
13. Zheng, G., A. A. Kishk, A. W. Glisson, and A. B. Yakovlev, "Simplified feed for modified printed Yagi antenna," *Electron. Lett.*, Vol. 40, No. 8, 464–466, Apr. 2004.
14. Shiroma, G. S. and W. A. Shiroma, "A two-element L-band Quasi-Yagi antenna array with omnidirectional coverage," *IEEE Trans. Antennas Propag.*, Vol. 55, No. 12, 3713–3716, Dec. 2007.
15. Kan, H. K., R. B. Waterhouse, A. M. Abbosh, and M. E. Bialkowski, "Simple broadband planar CPW-fed Quasi-Yagi antenna," *IEEE Antennas Wireless Propag. Lett.*, Vol. 6, 18–20, 2007.
16. Lin, S., G.-L. Huang, R.-N. Cai, and J.-X. Wang, "Novel printed Yagi-Uda antenna with highgain and broadband," *Progress In Electromagnetics Research Letters*, Vol. 20, 107–117, 2011.
17. Estrada, J. G., C. I. Páez, and A. Fajardo, "A new broadband quasi Yagi-Uda antenna with an EBG-truncated ground plane," *IEEE Antennas Wireless Propag. Lett.*, Vol. 12, 1392–1395, 2013.
18. Yeo, J. and J.-I. Lee, "Bandwidth enhancement of double-dipole Quasi-Yagi antenna using stepped slotline structure," *IEEE Antennas Wireless Propag. Lett.*, Vol. 15, 694–697, 2016.
19. Farran, M., et al., "Compact Quasi-Yagi antenna with folded dipole fed by tapered integrated balun," *Electron. Lett.*, Vol. 52, No. 10, 789–790, May 2016.
20. Luo, Y., Q. X. Chu, and J. Bornemann, "A differential-fed Yagi-Uda antenna with enhanced bandwidth via addition of parasitic resonator," *Microw. Opt. Technol. Lett.*, Vol. 59, No. 1, 156–159, Jan. 2017.
21. Chu, H., Y.-X. Guo, H. Wong, and X. Shi, "Wideband self-complementary Quasi-Yagi antenna for millimeter-wave systems," *IEEE Antennas Wireless Propag. Lett.*, Vol. 10, 322–325, 2011.
22. Liang, Z., J. Liu, Y. Zhang, and Y. Long, "A novel microstrip quasi Yagi array antenna with annular sector directors," *IEEE Trans. Antennas Propag.*, Vol. 63, No. 10, 4524–4529, Oct. 2015.
23. Huang, E. and T. Chiu, "Printed Yagi antenna with multiple reflectors," *Electron. Lett.*, Vol. 40, No. 19, 1165–1166, Sep. 2004.
24. Wu, J., Z. Zhao, Z. Nie, and Q.-H. Liu, "Bandwidth enhancement of a planar printed Quasi-Yagi antenna with size reduction," *IEEE Trans. Antennas Propag.*, Vol. 62, No. 1, 463–467, Jan. 2014.
25. Luo, Y. and Q.-X. Chu, "A Yagi-Uda antenna with a stepped-width reflector shorter than the driven element," *IEEE Antennas Wireless Propag. Lett.*, Vol. 15, 564–567, 2016.
26. Ding, K., C. Gao, B. Zhang, Y. Wu, and D. Qu, "A compact printed unidirectional broadband antenna with parasitic patch," *IEEE Antennas Wireless Propag. Lett.*, Vol. 16, 2341–2344, 2017.
27. Jehangir, S. S. and M. S. Sharawi, "A miniaturized UWB biplanar Yagi like MIMO antenna system," *IEEE Antennas Wireless Propag. Lett.*, Vol. 16, 2320–2323, 2017.
28. Kumar, H. and G. Kumar, "A broadband planar modified Quasi-Yagi using log-periodic antenna," *Progress In Electromagnetics Research Letters*, Vol. 73, 23–30, 2018.
29. Chopra, R. and G. Kumar, "Uniplanar microstrip antenna for endfire radiation," *IEEE Trans. Antennas Propag.*, Vol. 67, No. 5, 3422–3426, May 2019.
30. Solanki, R., "Compact and broadband uniplanar Yagi MSA for sub-6 GHz 5G frequency band," *2021 15th European Conference on Antennas and Propagation (EuCAP)*, 1–5, 2021, doi: 10.23919/EuCAP51087.2021.9411309.

31. Gheethan, A. A. and D. E. Anagnostou, "The design and optimization of planar LPDAs," *PIERS Online*, Vol. 4, No. 8, 811–814, 2008.
32. Anagnostou, D. E., J. Papapolymerou, M. M. Tentzeris, and C. G. Christodoulou, "A printed log-periodic koch-dipole array (LPKDA)," *IEEE Antennas Wireless Propag. Lett.*, Vol. 7, 456–460, 2008.
33. Song, L., Y. Nie, and J. Wang, "A novel meander line microstrip log-periodic dipole antenna for dual-polarized radar systems," *Progress In Electromagnetics Research Letters*, Vol. 56, 123–128, 2015.
34. Jardon-Aguilar, H., J. A. Tirado-Mendez, R. Flores-Leal, and R. Linares-Miranda, "Reduced log-periodic dipole antenna using a cylindrical-hat cover," *IET Microwaves, Antennas* & *Propagation*, Vol. 5, No. 14, 1697–1702, Nov. 18, 2011.
35. Casula, G. A., P. Maxia, G. Mazzarella, and G. Montisci, "Design of a printed log-periodic dipole array for ultra-wideband applications," *Progress In Electromagnetics Research C*, Vol. 38, 15–26, 2013.
36. Lei, F., Z. Li, Q.-X. Guo, H. Zhang, X. Zhang, J. Wang, Gu. Liu, J.-H. Wang, and Y. L. Yang, "A monolayer multi-octave bandwidth log-periodic microstrip antenna," *Progress In Electromagnetics Research Letters*, Vol. 41, 97–104, 2013.
37. Zhai, G. H., Y. Cheng, D. Min, S. Z. Zhu, and J. J. Gao, "Wideband simplified feed for printed log-periodic dipole array antenna," *Electron. Lett.*, Vol. 49, No. 23, 1430–1432, Nov. 2013.
38. Mirzapour, M. I., S. M. J. Razavi, and S. H. M. Armaki, "Ultra-wideband planar LPDA antenna with mode converter balun," *Electron. Lett.*, Vol. 50, No. 12, 848–850, Jun. 5, 2014.
39. Qu, S. W., J. L. Li, Q. Xue, and C. H. Chan, "Wideband periodic endfire antenna with bowtie dipoles," *IEEE Antennas Wireless Propag. Lett.*, Vol. 7, 314–317, 2008.
40. Gao, X., Z. Shen, and C. Hua, "Conformal VHF log-periodic balloon antenna," *IEEE Trans. Antennas Propag.*, Vol. 63, No. 6, 2756–2761, Jun. 2015.
41. Kyei, D., U. Sim, and Y. B. Jung, "Compact log-periodic dipole array antenna with bandwidth-enhancement techniques for the low frequency band," *IET Microwaves, Antennas* & *Propagation*, Vol. 11, No. 5, 711–717, Apr. 2017.
42. Zhai, G., et al., "Gain-enhanced planar log-periodic dipole array antenna using nonresonant metamaterial," *IEEE Trans. Antennas Propag.*, Vol. 67, No. 9, 6193–6198, Sept. 2019.